PHYSICAL REVIEW A

STATISTICAL PHYSICS, PLASMAS, FLUIDS, AND RELATED INTERDISCIPLINARY TOPICS

THIRD SERIES, VOLUME 43, NUMBER 8 15 APRIL 1991

Influence of asymmetry on multifractal properties of maps

M. G. Cosenza and J. B. Swift

Center for Nonlinear Dynamics and Department of Physics, University of Texas at Austin, Austin, Texas 78712

(Received 9 October 1990)

It is shown that the multifractal properties of a period-doubling attractor and of repellers associated with symmetric unimodal maps are affected if an asymmetry is introduced in the zth derivative of the map at its maximum of order z. For a quadratic map, a universal scaling factor associated with the period-doubling attractor is calculated as a function of an asymmetry parameter. Expansions of multifractal functions in terms of an asymmetry parameter are obtained.

The multifractal analysis[1] has been established as a very convenient representation of the scaling properties of fractal measures. It consists in covering a set with N boxes of radii $\{l_i\}_{i=1}^N$, each having a probability p_i, which scales as $p_i \sim l_i^{\alpha}$ in the limit $l_i \to 0$, in order to construct a partition function

$$\Gamma(q,\tau,\{l_i\}) = \sum_{i=1}^{N} \frac{p_i^q}{l_i^{\tau}} . \tag{1}$$

The requirement $\lim_{N\to\infty}\Gamma = 1$ determines the function $\tau(q)$, which in turn yields the function $f(\alpha)$ through a Legendre transform. $f(\alpha)$ can be interpreted as the fractal dimension of the subset of the measure having scaling index α. The generalized dimensions[2] D_q are then related to $\tau(q)$ by $\tau(q) = (q-1)D_q$. One of the most important theoretical and experimental applications of this formalism has been the characterization of attractors arising in dynamical systems.[1,3,4] Specifically, much interest has been dedicated to one-parameter, unimodal maps of the type

$$x_{n+1} = f(x_n) = 1 - a|x_n|^z , \tag{2}$$

where $x \in [-1,1]$, $a > 0$, and $z \geq 1$.

Recent numerical and experimental work[5-7] has shown that the metric universality associated with the sequence of period-doubling bifurcations is strongly affected when an asymmetry is introduced at the maximum of a map. In this paper we examine the behavior of multifractal properties of a repeller and a period-doubling attractor, both obtained from Eq. (2), when an asymmetry in the amplitude a is considered (discontinuity of the zth derivative at the maximum).

For $z = 1$, an asymmetric tent map can be defined by

$$f(x_n) = \begin{cases} 1 + a x_n, & x_n < 0 \\ 1 - b x_n, & x_n > 0 , \end{cases} \tag{3}$$

where $a, b > 1$ and $a^{-1} + b^{-1} < 1$ so that a repeller appears. After n iterations of the map, the repelling set consists of $N = 2^n$ intervals, $n!/[m!(n-m)!]$ of which have the same normalized length $l_m = a^{-m} b^{-(n-m)}$. We assume probability distributions on the geometric support of the repeller described by Gibbs measures of the form[8] $p_i = l_i^s / \sum_i l_i^s$. The cases $s = 0$, uniform probability, and $s = 1$, geometrical multifractality, are physically relevant and can be achieved under specific initial conditions.[8]

For a uniform measure, $p_i = 2^{-n}$, the partition function Eq. (1) can be expressed as a binomial product,

$$\Gamma_n(q,\tau) = 2^{-nq} \sum_{m=0}^{n} \frac{n!}{m!(n-m)!} (l_m)^{-\tau} = [2^{-q}(a^{\tau} + b^{\tau})]^n . \tag{4}$$

The asymmetry can be quantified with the parameter

$$\gamma = \frac{b-a}{b+a} , \quad -1 \leq \gamma \leq 1 \tag{5}$$

and to characterize the expanding properties of the map, we introduce the parameter

$$\epsilon = \frac{ab}{a+b} - 1 , \quad \epsilon \geq 0 \tag{6}$$

which is related to the escape rate of the repeller, defined as[9]

$$r=\lim_{n\to\infty}\frac{1}{n}\ln\left[\sum_{i=1}^{2^n} l_i\right], \tag{7}$$

and in this case given by $r=\ln(1+\epsilon)$. By setting $\Gamma_n=1$, we get in terms of γ and ϵ,

$$(1+\gamma)^{-D_q(q-1)}+(1-\gamma)^{-D_q(q-1)}=2^q[2(1+\epsilon)]^{-D_q(q-1)}. \tag{8}$$

For fixed q and ϵ, Eq. (8) determines $D_q(\gamma)$, which has the obvious symmetry $D_q(\gamma)=D_q(-\gamma)$. When $\gamma=0$, the repelling set is a simple fractal, with fractal dimension independent of q,

$$D_q(0)=\frac{\ln 2}{\ln[2(1+\epsilon)]}. \tag{9}$$

Note that if $D_q(q-1)=-1$, then Eq. (8) yields a value

$$\bar{q}=-\frac{\ln(1+\epsilon)}{\ln 2}, \tag{10}$$

for which $D_{\bar{q}}(\gamma)=D_q(0)$, i.e., the generalized dimension corresponding to this particular value of q is unchanged by the asymmetry of the map. Further, we find that for finite q, $[dD_q/d\gamma]_{\gamma=0}=0$, and therefore a Taylor expansion of $D_q(\gamma)$ around $\gamma=0$ gives

$$D_q(\gamma)=D_q(0)-\frac{D_q^2(0)[D_q(0)(q-1)+1]}{\ln 2}\gamma^2+\cdots. \tag{11}$$

Figure 1 shows D_q versus γ for several values of q. For a uniform probability density ($s=1$), the requirement $\Gamma_n=1$ determines $D_q(\gamma)$, which in this situation has the Taylor expansion

$$D_q(\gamma)=D_q(0)-\frac{[1-D_q(0)][q-D_q(0)(q-1)]}{\ln 2}\gamma^2+\cdots. \tag{12}$$

The condition $D_q(q-1)=q$ implies a value $\bar{q}=-\ln 2/\ln(1+\epsilon)$, for which $D_{\bar{q}}(\gamma)=D_q(0)$. When $\epsilon\to 0$, both Eqs. (11) and (12) give the scaling

$$D_q(\epsilon,\gamma)\sim\left[1-\frac{\epsilon}{\ln 2}\right]-c(q)\epsilon\gamma^2, \tag{13}$$

where $c(q)$ is a function of q.

As a next example, consider the quadratic map $x_{n+1}=f_{a,b}(x_n)$ given by

$$f_{a,b}(x_n)=\begin{cases}1-ax_n^2, & x_n\le 0\\ 1-bx_n^2, & x_n\ge 0.\end{cases} \tag{14}$$

We define a curve $\lambda_n(a,b)$ as the set of values of a and b for which a superstable orbit of period 2^n exists. By using the word lifting method introduced in Ref. 10, the curves $\lambda_n(a,b)$ can be calculated for successive n. The sequence $\{\lambda_n(a,b)\}$ converges to a curve $\lambda_\infty(a,b)$, which determines the accumulation of period-doubling bifurcations and the first onset of chaos in the space of parameters (a,b). Figure 2 shows $\lambda_2(a,b)$ and the asymptotic $\lambda_\infty(a,b)$. The convergence rate to each point $(a_\infty,b_\infty)\in\lambda_\infty(a,b)$ presents an oscillatory behavior, for increasing n, between two constants[6,11] $\delta_1=\delta_1(a_\infty,b_\infty)$ and $\delta_2=\delta_2(a_\infty,b_\infty)$. If we define the points $(a_n,b_n)\in\lambda_n(a,b)$ such that $b_n/a_n=b_\infty/a_\infty$, for all n these constants can be expressed as

$$\delta_1=\lim_{n\to\infty}\frac{a_{2n}-a_{2n-1}}{a_{2n+1}-a_{2n}}, \tag{15}$$

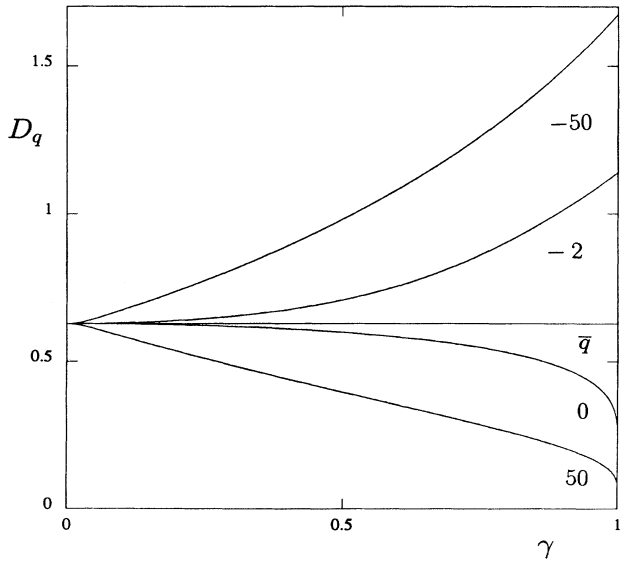

FIG. 1. Dependence of D_q with the asymmetry parameter γ, in the case of a linear map with uniform probability. The number below each curve indicates the value of q. Here, $\epsilon=0.5$ and $\bar{q}=-0.585$, given by Eq. (10).

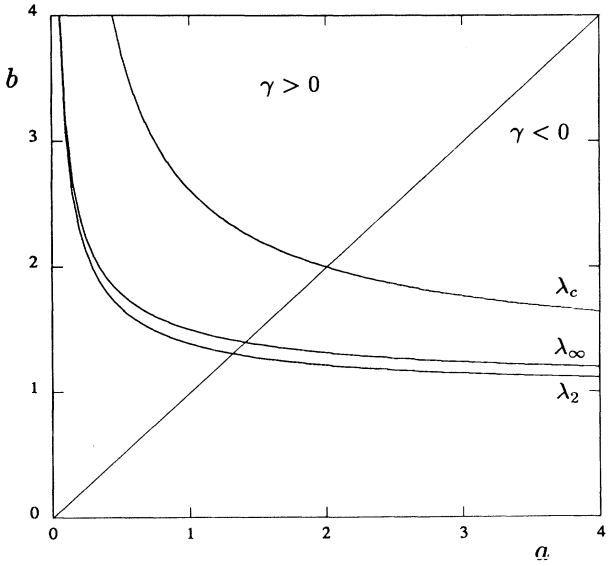

FIG. 2. Critical curves in the plane (a,b). λ_2, superstable orbit of period 2^2; λ_∞, accumulation of period-doubling bifurcations; λ_c, fully developed chaos. The curves are not symmetric under the exchange of a and b. The sign of the asymmetry parameter is indicated on each region.

$$\delta_2 = \lim_{n\to\infty} \frac{a_{2n+1}-a_{2n}}{a_{2n+2}-a_{2n+1}} , \tag{16}$$

or, equivalently, in terms of the b_n's. The 2^n superstable cycle corresponding to a pair (a_n,b_n) is generated by the iterates

$$x_i(a_n,b_n) = f^{(i)}_{a_n,b_n}(0) , \quad i=1,\ldots,2^n \tag{17}$$

and the intervals between adjacent iterates have the form

$$l_i(a_n,b_n) = |x_i(a_n,b_n) - x_{i+2^{n-1}}(a_n,b_n)| , \quad i=1,\ldots,2^{n-1} \tag{18}$$

the largest and the smallest of which are $l_{\max}(a_n,b_n) = l_{2^{n-1}}(a_n,b_n)$ and $l_{\min}(a_n,b_n) = l_1(a_n,b_n)$, respectively. The probabilities p_i of the intervals are all equal.

An oscillatory behavior is also observed for scaling factor $\alpha(n) = l_{\max}(a_n,b_n)/l_{\max}(a_{n+1},b_{n+1})$. There are two limit values for $\alpha(n)$ as $n\to\infty$, given by

$$\alpha_1 = \lim_{n\to\infty} \frac{l_{\max}(a_{2n},b_{2n})}{l_{\max}(a_{2n+1},b_{2n+1})} , \tag{19}$$

$$\alpha_2 = \lim_{n\to\infty} \frac{l_{\max}(a_{2n+1},b_{2n+1})}{l_{\max}(a_{2n+2},b_{2n+2})} . \tag{20}$$

Each accumulation point (a_∞,b_∞) is characterized by factors δ_1,δ_2 and α_1,α_2. It has been shown[12] that at (a_∞,b_∞) there is a function $\bar{g}(x)$ satisfying the equation

$$\sigma \bar{g}^{(4)}(x/\sigma) = \bar{g}(x) , \tag{21}$$

where both $\sigma = \alpha_1\alpha_2$ and $\bar{g}(x)$ depend on (a_∞,b_∞). Here we introduce the asymmetry variable

$$\gamma = \frac{b_\infty - a_\infty}{b_\infty + a_\infty}, \quad -1 \le \gamma \le 1 \tag{22}$$

which parametrizes the curve $\lambda_\infty(a,b)$, and investigate the behavior of $\sigma(\gamma)$. Figure 3 shows σ calculated numerically from Eqs. (19) and (20), as a function of γ. The quantity σ has the property $\sigma(\gamma)=\sigma(-\gamma)$ and presents a minimum at $\gamma=0$, with the value $\sigma(0)=\alpha_{pd}^2$, where $\alpha_{pd}=2.5029\ldots$ is the scaling factor for symmetric quadratic maps.[13] In order to study the multifractal properties of the period-doubling attractor along the curve $\lambda_\infty(a,b)$, we first consider the dimensions $D_{\pm\infty}(\gamma)$, as $\gamma\to 0$. In the limit $n\to\infty$, Eqs. (19) and (20) imply that $l_{\max}\sim\sigma^{-n/2}$ and, since the map is quadratic around its maximum, $l_{\min}\sim\sigma^{-n}$. Therefore, for $\gamma\to 0$, the condition $\Gamma_n = 1$ gives

$$D_{-\infty}(\gamma) = \frac{\ln p_i}{\ln l_{\max}} \simeq \frac{\ln 2}{\ln \alpha_{pd}} \left[1 - \frac{c\gamma^2}{2\alpha_{pd}^2 \ln \alpha_{pd}} \right] , \tag{23}$$

$$D_{+\infty}(\gamma) = \frac{\ln p_i}{\ln l_{\min}} \simeq \frac{\ln 2}{2\ln \alpha_{pd}} \left[1 - \frac{c\gamma^2}{2\alpha_{pd}^2 \ln \alpha_{pd}} \right] , \tag{24}$$

where $c \equiv (d^2\sigma/d\gamma^2)_{\gamma=0} \approx 1.076$. These results suggest the following scaling for the deviation of any dimension $D_q(\gamma)$, for small γ, from its value at symmetry

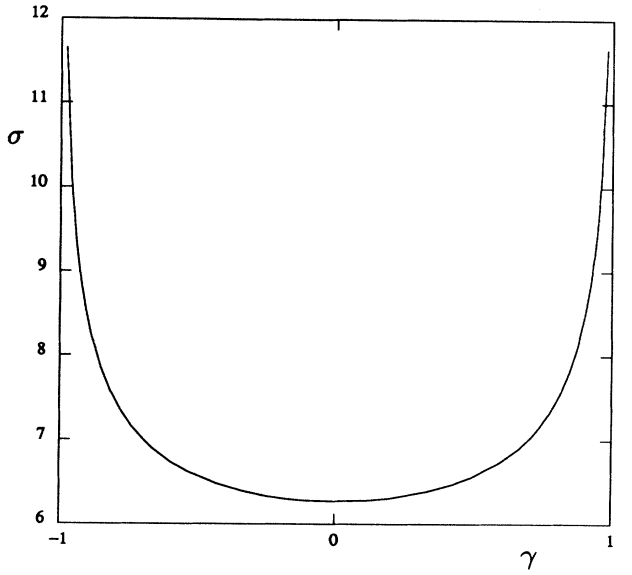

FIG. 3. The scaling factor $\sigma = \alpha_1\alpha_2$, obtained numerically, as a function of γ.

$$D_q(0) - D_q(\gamma) \simeq C_q\gamma^2 , \tag{25}$$

where $C_q = (d^2D_q/d\gamma^2)_{\gamma=0}$. Figure 4 presents several D_q, calculated numerically with l_i given by Eq. (18), versus γ, showing the symmetry $D_q(\gamma) = D_q(-\gamma)$. The scaling Eq. (25) is verified in Fig. 5, where D_q is shown as a function of γ^2, for different q.

The curve $\lambda_c(a,b)$ of Fig. 2 is given by $b = a(b-1)^2$, and it corresponds to the condition of crisis, or fully developed chaos, i.e., to the values of a and b for which $f_{a,b}$ maps an interval $[\xi,1]$ onto itself. For values of a and b above the curve $\lambda_c(a,b)$,the iteration of $f_{a,b}$ generates a repeller. We define a parameter

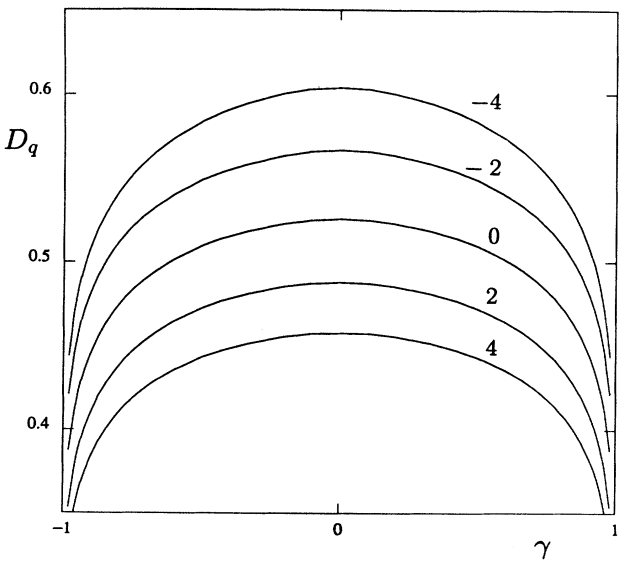

FIG. 4. D_q as a function of γ, for the map Eq. (14). Several values of q are indicated.

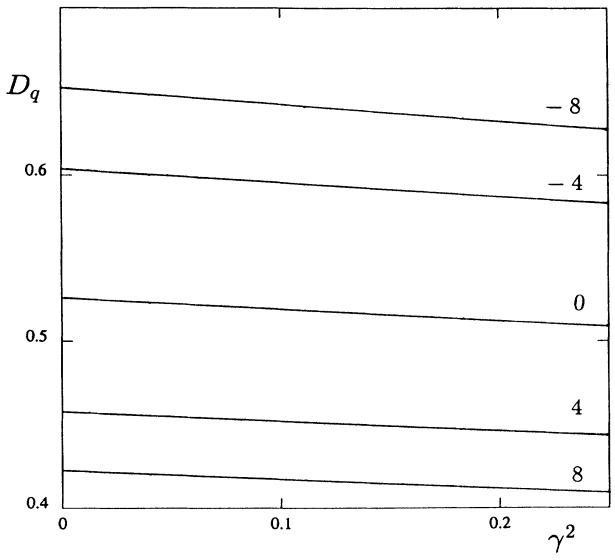

FIG. 5. D_q as a function of γ^2, for several values of q.

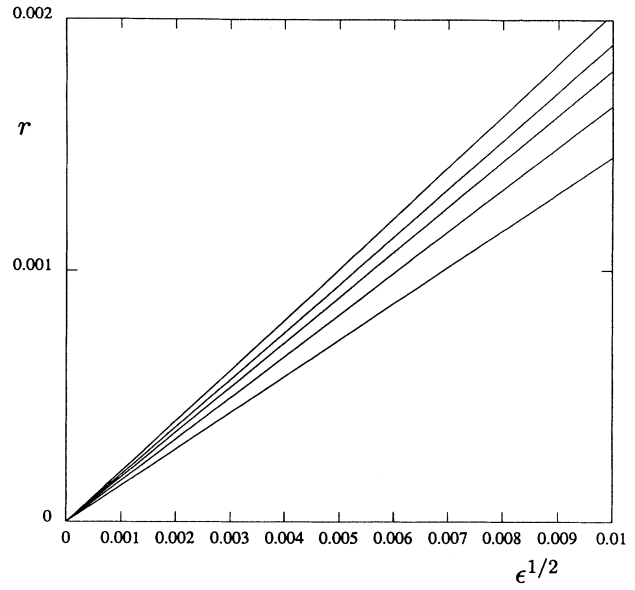

FIG. 6. The escape rate, Eq. (7), as a function of $\epsilon^{1/2}$ for several values of γ. From top to bottom, the curves correspond to $\gamma=0.95$, 0.6, 0, -0.6, and -0.95.

$$\epsilon=\frac{a}{b}(b-1)^2-1, \quad \epsilon>0 , \tag{26}$$

in addition to γ, Eq. (5), and investigate the behavior of the escape rate, Eq. (7), as a function of ϵ and γ. As in the symmetric case,[14] it is the order z of the map at its maximum that determines the scaling of the escape rate as $r\sim\epsilon^{1/z}$, when $\epsilon\to 0$. For a map such as Eq. (14), we expect the following scaling of r:

$$r=h(\gamma)\epsilon^{1/2} , \tag{27}$$

where $h(\gamma)$ is a function of the asymmetry parameter γ. The escape rate can be calculated from its definition, Eq. (7), as a function of ϵ, for fixed γ. Figure 6 shows r versus $\epsilon^{1/2}$, for different values of γ, confirming Eq. (27). The slopes of the lines in Fig. 6 give the asymmetry function $h(\gamma)$. This function is plotted in Fig. 7. Around $\gamma=0$, $h(\gamma)$ can be expanded as $h(\gamma)=c_1+c_2\gamma$, with $c_1\approx 0.1804$ and $c_2\approx 0.025$ numerically found. As shown in Ref. 15, the escape rate enters naturally in the partition function Eq. (1), and it determines the scaling properties of the multifractal functions for repellers generated by one-dimensional maps. For a uniform probability density ($s=1$), for example, the generalized dimensions D_q behave as[15] $1-D_q\sim A(q)r$, close to the crisis condition. Therefore, the corresponding scaling in the presence of asymmetry must have the form

$$1-D_q(\epsilon,\gamma)\sim a(q)(c_1+c_2\gamma)\epsilon^{1/2} , \tag{28}$$

for both $\epsilon\to 0$ and $\gamma\to 0$. The condition $D_q(q-1)=q$ selects a value $\bar{q}=\ln 2/r$, as in the $z=1$ case, but the behavior of the escape rate now causes all D_q's (including $D_{\bar{q}}$) to depend on both ϵ and γ.

In conclusion, we have shown how a small asymmetry in the amplitude of a map at its maximum affects the multifractal properties of associated attractors or repellers. In the case of an asymmetric quadratic map, we have calculated the universal scaling factor $\sigma\equiv\alpha_1\alpha_2$, which describes the metric properties of the period-doubling attractor, as a function of an asymmetry parameter γ. The function $\sigma(\gamma)$ influences the scaling of the generalized dimensions of the attractor, with the result that a small asymmetry appears as a second-order effect in the D_q's. For a repeller generated by a quadratic map close to the crisis condition, the escape rate rules the scaling properties of the multifractal quantities and its depen-

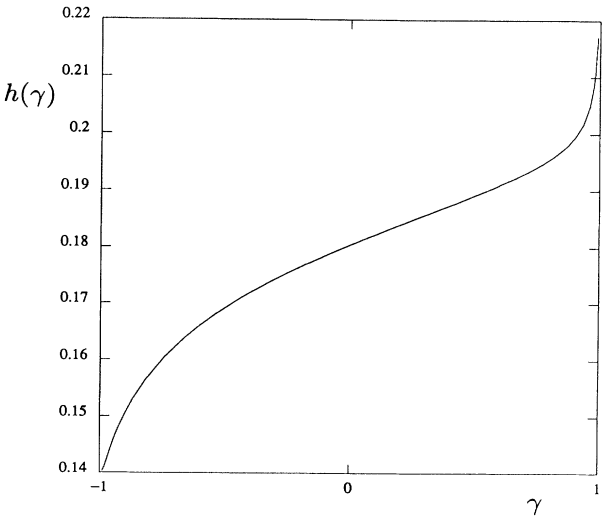

FIG. 7. The function $h(\gamma)$ in Eq. (27), obtained from the slopes of the lines in Fig. 6.

dence on the asymmetry parameter was numerically established. When the parameter is small, the dimensions D_q depend linearly on it. We have shown that, for a two-scale Cantor set repeller generated by an asymmetric linear map, the asymmetry also appears as a second-order correction to the corresponding D_q's of the symmetric case. Experimentally obtained functions D_q or $f(\alpha)$ have been modeled by the resulting multifractal properties of maps or two-scale Cantor sets.[4,3,16] The knowledge of the behavior of multifractal functions associated with maps when some parameters are varied can be relevant when comparing theoretical models with the experimental measurements of these functions.

We are grateful to Professor Hao Bai-Lin for useful suggestions. This work was supported in part by the U.S. Department of Energy under Grant No. DE-FGO5-88ER 13821.

[1]T. C. Halsey, M. H. Jensen, L. P. Kadanoff, I. Procaccia, and B. I. Shraiman, Phys. Rev. A **33**, 1141 (1986).
[2]G. E. Hentschel and I. Procaccia, Physica D **8**, 435 (1983).
[3]M. H. Jensen, L. P. Kadanoff, A. Libchaber, and J. Stavans, Phys. Rev. Lett. **55**, 2798 (1985).
[4]J. A. Glazier, M. H. Jensen, A. Libchaber, and J. Stavans, Phys. Rev. A **34**, 1621 (1986).
[5]M. C. de Sousa Vieira and C. Tsallis, Europhys. Lett. **9**, 119 (1989).
[6]M. C. de Sousa Vieira, Phys. Lett. A **143**, 279 (1990).
[7]M. Octavio, A. Da Costa, and J. Aponte, Phys. Rev. A **34**, 1512 (1986).
[8]J. L. McCauley, Int. J. Mod. Phys. B **3**, 821 (1989).
[9]L. P. Kadanoff and C. Tang, Proc. Nat. Acad. Sci. U.S.A. **81**, 1276 (1984).
[10]Zeng Wan-Zhen and Hao Bai-Lin, Commun. Theor. Phys. **3**, 283 (1984).
[11]A. Arneodo, P. Coullet, and C. Tresser, Phys. Lett. A **70**, 74 (1979).
[12]H. Kawai and S. H. H. Tye, Phys. Rev. A **30**, 2005 (1984).
[13]M. J. Feigenbaum, J. Stat. Phys. **19**, 25 (1978).
[14]O. B. Christensen and T. Bohr, Phys. Scr. **38**, 641 (1988).
[15]M. G. Cosenza and J. B. Swift, Phys. Rev. A **41**, 6615 (1990).
[16]C. Meneveau and K. R. Sreenivasan, Phys. Rev. Lett. **59**, 1424 (1987).